Development 137, 3417-3426 (2010) doi:10.1242/dev.051789

Preaxial polydactyly: interactions among ETV, TWIST1 and HAND2 control anterior-posterior patterning of the limb

Zhen Zhang[1], Pengfei Sui[2], Aiwu Dong[2], John Hassell[3], Peter Cserjesi[4], You-Tzung Chen[5], Richard R. Behringer[5] and Xin Sun[1,*]

SUMMARY

Preaxial polydactyly (PPD) is a common limb-associated birth defect characterized by extra digit(s) in the anterior autopod. It often results from ectopic sonic hedgehog (*Shh*) expression in the anterior limb bud. Although several transcription factors are known to restrict *Shh* expression to the posterior limb bud, how they function together remains unclear. Here we provide evidence from mouse conditional knockout limb buds that the bHLH family transcription factor gene *Twist1* is required to inhibit *Shh* expression in the anterior limb bud mesenchyme. More importantly, we uncovered genetic synergism between *Twist1* and the ETS family transcription factor genes *Etv4* and *Etv5* (collectively Etv), which also inhibit *Shh* expression. Biochemical data suggest that this genetic interaction is a result of direct association between TWIST1 and ETV proteins. Previous studies have shown that TWIST1 functions by forming homodimers or heterodimers with other bHLH factors including HAND2, a key positive regulator of *Shh* expression. We found that the PPD phenotype observed in Etv mutants is suppressed by a mutation in *Hand2*, indicative of genetic antagonism. Furthermore, overexpression of ETV proteins influences the dimerization of these bHLH factors. Together, our data suggest that through biochemical interactions, the *Shh* expression regulators ETV, TWIST1 and HAND2 attain a precise balance to establish anterior-posterior patterning of the limb.

KEY WORDS: Anterior-posterior patterning, Limb development, Sonic hedgehog signaling, Mouse

INTRODUCTION

The developing limb is an excellent model for studying pattern formation because construction of the limb skeleton follows a blueprint laid down in the early embryonic limb bud. Several signaling centers are responsible for precise formation of this three-dimensional structure (Niswander, 2002; Zeller et al., 2009). In particular, the anterior-posterior (A-P; thumb to little finger) axis of the limb is patterned by the zone of polarizing activity (ZPA), a group of mesenchymal cells near the posterior margin of the limb bud. These cells produce the secreted molecule sonic hedgehog (SHH), which is crucial for limb A-P patterning. Altering the level or location of *Shh* gene expression results in changes in the number and/or identity of digits. For example, ectopic expression of *Shh* in the anterior limb bud leads to preaxial polydactyly (PPD; the formation of extra digits anteriorly) in mice, which resembles a common limb-associated human birth defect of the same name. Thus, tight regulation of *Shh* expression is crucial for normal A-P patterning of the limb (McGlinn and Tabin, 2006).

Control of *Shh* expression in the limb bud is achieved through a cis-element called the ZPA regulatory sequence (ZRS), located ~1 Mb upstream of the *Shh* promoter (Lettice et al., 2003; Maas and Fallon, 2005; Sagai et al., 2005). The ZRS is necessary and sufficient to promote *Shh* expression specifically in the limb bud, but not elsewhere in the developing embryo. In addition, multiple point mutations scattered across the ZRS are individually linked to ectopic *Shh* expression in the anterior limb bud (Lettice et al., 2003; Maas and Fallon, 2005; Gurnett et al., 2007; Furniss et al., 2008), suggesting that the ZRS also mediates the repression that is essential for restricting *Shh* expression to the posterior limb bud. Although a number of transcription factors have been shown to regulate *Shh* expression in the limb bud (Buscher et al., 1997; Bourgeois et al., 1998; Qu et al., 1998; Zhang et al., 2009), few have been demonstrated to directly bind the ZRS (Capellini et al., 2006; Galli et al., 2010).

Factors that control *Shh* expression in the limb bud can be characterized as either positive or negative regulators based on their mutant phenotypes. For example, loss-of-function mutants in *Alx4*, *Gli3* and *Twist1* display ectopic expression of *Shh* in the anterior limb bud, indicating that these genes normally inhibit *Shh* expression in this region (Buscher et al., 1997; Bourgeois et al., 1998; Qu et al., 1998). Loss-of-function mutants in *Hand2*, *Hox10-13*, *Tbx3* and *Pbx1;2* display reduced or absent *Shh* expression in the posterior limb bud, indicating that they normally activate *Shh* expression in this region (Charite et al., 2000; Davenport et al., 2003; Capellini et al., 2006; Tarchini et al., 2006). There is a substantial overlap in the expression patterns of many of these factors, raising the possibility that the normal posterior restriction of *Shh* expression may be achieved through compound interactions among these positive and negative regulators, acting either directly or indirectly on the ZRS.

The genetic and biochemical relationships among these *Shh* regulators are beginning to be elucidated (te Welscher et al., 2002; Chen et al., 2004; Firulli et al., 2005; Vokes et al., 2008). For example, HAND2 and TWIST1, two *Shh* regulators belonging to the basic helix-loop-helix (bHLH) family, antagonize each other by

[1]Laboratory of Genetics, University of Wisconsin-Madison, Madison, WI 53706, USA. [2]State Key Laboratory of Genetic Engineering, Department of Biochemistry, School of Life Sciences, Fudan University, Shanghai 200433, China. [3]Department of Biochemistry and Biomedical Sciences, McMaster University, Hamilton, ON L8N 3Z5, Canada. [4]Department of Pathology and Cell Biology, Columbia University, New York, NY 10032, USA. [5]Department of Genetics, University of Texas M.D. Anderson Cancer Center, Houston, TX 77030, USA.

*Author for correspondence (xsun@wisc.edu)

Accepted 2 August 2010

forming protein heterodimers (Firulli et al., 2005). Data from knockout, overexpression and chromatin immunoprecipitation (ChIP) experiments are consistent with the conclusion that HAND2 acts as a key positive regulator of *Shh* expression in the limb bud (Charite et al., 2000; Fernandez-Teran et al., 2000; Galli et al., 2010). By contrast, there are conflicting data on the role of TWIST1 in regulating *Shh* expression. *Twist1* heterozygous mutants exhibit hindlimb-specific PPD and ectopic *Shh* expression, suggesting that TWIST1 inhibits *Shh* expression (Bourgeois et al., 1998). However, *Twist1* homozygous limb buds show overall diminished *Shh* expression, suggesting that TWIST1 is required for *Shh* expression (O'Rourke et al., 2002; Zuniga et al., 2002). This downregulation of *Shh* could be due to disruption of the apical ectodermal ridge (AER) observed in *Twist1* homozygous limb buds. We investigate this possibility here by bypassing the requirement for *Twist1* in AER formation. Our data from *Twist1* conditional homozygous mutants suggest that, at a stage after the establishment of the AER, TWIST1 is required for inhibiting *Shh* expression in the anterior limb bud of both the forelimb and hindlimb.

Recent studies, including one from our laboratory, show that two PEA3 group ETS domain-containing transcription factors, ETV4 and ETV5 (hereafter ETV proteins), function as negative regulators of *Shh* expression (Mao et al., 2009; Zhang et al., 2009). Specifically, we found that limb-specific inactivation of both Etv genes led to ectopic *Shh* expression in the anterior limb bud and to PPD. We sought to address how they function together with the other known *Shh* regulators listed above. In this study, we report genetic and biochemical evidence suggesting that ETV inhibits *Shh* expression by regulating the dimerization of TWIST1/HAND2.

MATERIALS AND METHODS

Mouse mutant phenotype analyses

Embryos were dissected from time-mated mice, counting noon on the day the vaginal plug was found as E0.5. Mutant and transgenic alleles used in this study have been described previously: *Twist1*^{F} (Chen et al., 2007), *Twist1*^{Ska10} (Bialek et al., 2004), *Etv4*$^{-}$ (Livet et al., 2002), *Etv5*^{F} (Zhang et al., 2009), *Hand2*^{F} (Morikawa et al., 2007), *Prx1cre* (Logan et al., 2002) and *Tcre* (Perantoni et al., 2005). All mutants were generated in a mixed strain background. Although no genetic background effects were discerned, littermates were used to control for any possible differences due to background variations. Whenever possible, somite-matched mutant and control limb buds were used for comparisons. Whole-mount in situ hybridization was performed as described (Neubuser et al., 1997). Skeletal preparations were performed using Alcian Blue and Alizarin Red and a standard protocol.

His tag pull-down assay

Full-length mouse *Etv5* was cloned into the pET28a vector (Novagen) and the construct (pET-Etv5) was used to transform *E. coli.* strain BL21(DE3). To prepare bait protein samples, cultures of BL21(DE3) transformed by pET-Etv5 (His-ETV5) or pET28a (control) were induced by 1 mM IPTG at 16°C for 3 hours. The cells were then lysed using BugBuster Master Mix (Novagen). The supernatant of the lysate was mixed with Ni-NTA beads (Qiagen) at 4°C for 1 hour. After incubation, the beads were washed with wash buffer 1 [50 mM sodium phosphate (NaP), 150 mM NaCl, 40 mM imidazole, 0.1% Tween 20, 10% glycerol, 10 mM β-mercaptoethanol, pH 7.6] three times. To prepare the prey sample, HEK293T cells overexpressing Myc-TWIST1 were lysed with lysis buffer [20 mM NaP, 150 mM NaCl, 0.1% Triton X-100, 10% glycerol, 40 mM imidazole, Protease Inhibitor Cocktail (Sigma P8340, 1:100), Phosphatase Inhibitor Cocktail I (Sigma P2850, 1:100) pH 7.6]. The lysate was split equally into two tubes and mixed at 4°C for 2 hours with beads treated with ETV5 sample or control sample. Then, the beads were washed with wash buffer 1 three times and with wash buffer 2 (50 mM NaP, 200 mM NaCl, 40 mM imidazole, 1% Tween 20, 10% glycerol, 15 mM β-mercaptoethanol, pH 7.6) three times. Protein was eluted from the beads using 0.2 M glycine pH 2.5.

Generation of the ETV5 antibody

An *E. coli* BL21(DE3) culture transformed by pET-Etv5 was used to produce His-tagged ETV5 (His-ETV5). The culture at OD_{600} 0.6 was induced by 1 mM IPTG at 16°C for 3 hours. His-ETV5 protein was purified by Ni-NTA agarose (Qiagen) from the soluble fraction of the lysate and used to inject rabbits. The rabbit antiserum was commercially produced by Harlan Laboratories. Rabbits were boosted three times with freshly made His-ETV5 protein and the final bleed was used to purify the antibody against ETV5 by affinity chromatography using His-ETV5-coupled agarose beads. For pre-immune serum control, total IgG was purified using Protein A beads (Pharmacia) from a bleed prior to His-ETV5 injection. Equal amounts of the purified ETV5 antibody or pre-bleed IgG were coupled to Affi-Gel 10 (BioRad) for immunoprecipitation (IP).

Immunoprecipitation

Protein lysates for IP were prepared from HEK293T cells or mouse E11 limb buds. To prepare samples from cultured cells, HEK293T cells were transfected with plasmids containing Flag-tagged full-length or truncated *Etv5*, Myc-tagged *Hand2* or *Twist1*, or Flag-tagged *Twist1* by Lipofectamine 2000 (Invitrogen) following the manufacturer's protocol. Briefly, 3.6×10^{6} cells were plated per 100-mm dish 1 day before transfection. To test for ETV5 and TWIST1 interaction, *Etv5* plasmids (8 μg) and *Twist1* plasmids (8 μg) or empty vectors were mixed with 40 μl Lipofectamine 2000. To test for interaction between ETV5 and HAND2-TWIST1 dimers, Flag-tagged truncated *Etv5* plasmid (8 μg), Flag-tagged *Twist1* plasmid (4 μg), and Myc-tagged *Hand2* or *Twist1* (4 μg) were mixed with 40 μl Lipofectamine 2000. The mixture was added to the culture medium for transfection. About 48 hours post-transfection, the cells were lysed in 1 ml IP buffer [50 mM Tris pH 7.5, 150 mM NaCl, 0.1% Triton X-100, 10% glycerol, Protease Inhibitor Cocktail (1:100), Phosphatase Inhibitor Cocktail I (1:100)] per plate. For samples from limb buds, nuclear protein extract was prepared from 200 limb buds of E11 Swiss Webster mouse embryos using the NE-PER Nuclear and Cytoplasmic Extraction Kit (Pierce).

For IP from cell lysates, we used Protein G beads (Pharmacia). Cell lysates were mixed with antibodies and rotated for 2 hours at 4°C, then mixed with Protein G beads for 1 hour at 4°C. For IP from limb bud lysates, we used antibody-coupled Affi-Gel beads as described above. The lysates were diluted with IP buffer and split equally into two tubes. One was mixed with ETV5 antibody-coupled beads and the other with pre-immune IgG-coupled beads. The mixtures were rotated for 2 hours at 4°C. The beads were then washed four times with 1 ml wash buffer (50 mM Tris pH 7.5, 150 mM NaCl, 0.1% Tween 20, 10% glycerol). Protein was eluted from the beads using 0.1 M glycine pH 2.5. Western blot analysis was performed using the precipitated products.

Western blot analysis

Protein samples were run on 8-15% SDS-PAGE gels and transferred onto PVDF membrane. The membrane was blocked with 5% dried milk powder in TBST (50 mM Tris, 150 mM NaCl, 0.1% Tween 20, pH 7.6) for 1 hour, incubated with primary antibody at 4°C overnight, and with secondary antibody for 1 hour at room temperature. Visualization was carried out using ECL Plus reagents (GE Healthcare). The following primary antibodies were used: antigen-purified anti-ETV5 1:2500 (see above), anti-TWIST1 1:1000 (sc-81417, Santa Cruz Biotechnology), anti-HAND2 1:500 (AF3876, R&D), anti-MYF5 (sc-302, Santa Cruz), anti-Flag tag 1:1000 (F1804, Sigma) and anti-c-Myc tag 1:1000 (C3956, Sigma).

Yeast two-hybrid analysis

cDNAs encoding full-length or truncated ETV5, TWIST1 or HAND2 proteins without major activation domains were generated by RT-PCR (for primer sequences, see Table S1 in the supplementary material). The resulting PCR products were cloned into the pGEM-T vector (Promega) and sequence verified. These cDNAs were then subcloned into pGBKT7 and pGADT7 vectors (Clontech). Protein interactions were analyzed according to the manufacturer's recommendations (Clontech).

RESULTS

Bypassing the requirement for *Twist1* in AER formation reveals a requirement for *Twist1* in inhibiting *Shh* expression in the anterior limb bud

To investigate the relationship between Etv genes and other *Shh* regulators such as *Twist1*, we first clarified the role of *Twist1* in regulating *Shh* expression in the limb bud. In *Twist1* heterozygous mutants, *Shh* expression is not only present in the ZPA, but is also detected in the anterior mesenchyme of the hindlimb bud (O'Rourke et al., 2002). However, in *Twist1* homozygous mutants, *Shh* expression is diminished in the entire limb bud (O'Rourke et al., 2002; Zuniga et al., 2002). This reduced expression in *Twist1* homozygous mutants could be secondary to the reported failure to establish and maintain a normal AER. This role of *Twist1* in AER formation is likely to be indirect as *Twist1* is expressed in the limb bud mesenchyme. To bypass the requirement for *Twist1* in AER formation, we inactivated *Twist1* after limb bud initiation by combining *Prx1cre* with a floxed allele of *Twist1* (Logan et al., 2002; Chen et al., 2007), generating *Prx1cre;Twist1*$^{F/F}$ (hereafter referred to as *Prx1cre;Twist1*) mutants. Western blot analysis indicated that TWIST1 is present in mutant limb buds at a low level at E9.5, but is largely absent by E11 (Fig. 1A).

We found that in contrast to *Twist1*-null limb buds, the AER forms in *Prx1cre;Twist1* limb buds, as assessed by *Fgf8* expression (Fig. 1B-E). In *Prx1cre;Twist1* mutants, consistent with the presence of FGF in the AER, *Mkp3* (*Dusp6* – Mouse Genome Informatics) and *Spry4*, two downstream targets of FGF signaling, and *Fgfr1*, a principal FGF receptor, were expressed in the limb bud mesenchyme (see Fig. S1A-F in the supplementary material). Furthermore, *Fgf10*, a gene essential for AER formation, remained expressed in the mesenchyme of the *Prx1cre;Twist1* mutant limb bud (see Fig. S1G,H in the supplementary material), in contrast to its downregulation in *Twist1*-null limb buds (O'Rourke et al., 2002; Zuniga et al., 2002). These results suggest that the transient presence of TWIST1 at the beginning of limb bud initiation is sufficient to maintain the expression of key genes in the limb bud mesenchyme, which in turn allows for formation and maintenance of the AER in this conditional mutant.

In both the forelimb and hindlimb buds of *Prx1cre;Twist1* mutants, *Shh* was ectopically expressed in the anterior mesenchyme in addition to its expression in the ZPA (Fig. 1F-M and data not shown). In the forelimb bud, for example, the ectopic *Shh* domain started as a dot beneath the anterior margin of the AER at E10.5 (Fig. 1F-I), and expanded proximally past the extent of the AER by E11 (Fig. 1J-M). Even though the mutant limb buds were smaller than those of the control at these stages due to an earlier role of *Twist1* in cell survival (see Fig. S2 in the supplementary material), there was increased anterior regional growth by E12.5, possibly owing to the proliferative effect of ectopic SHH (data not shown). Also, as a consequence of the ectopic SHH, two downstream targets of SHH signaling, *Gli1* and *Ptch1*, were upregulated in the anterior mesenchyme (Fig. 1N-Q). Furthermore, the expression domains of *Fgf4* and gremlin 1 (*Grem1*), genes positively regulated by SHH signaling, were expanded anteriorly in both forelimb and hindlimb buds (Fig. 1R-U and data not shown). Consistent with the anterior expansion of *Fgf4*, the expression of *Mkp3* and *Spry4* was also expanded anteriorly (see Fig. S1A-D in the supplementary material). Compared with other known *Shh* inhibitor mutants, including those that we have analyzed, such as *Gli3*$^{-/-}$ and *Tcre;Etv4*$^{-/-}$*;Etv5*$^{F/-}$ (with inactivation of both *Etv4* and *Etv5* in the entire limb bud mesenchyme)

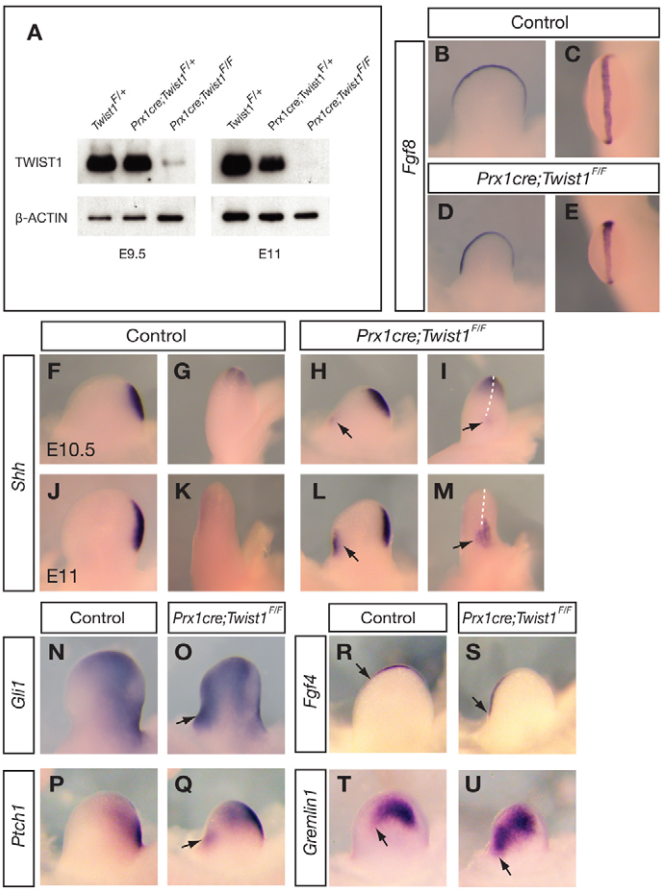

Fig. 1. Inactivation of TWIST1 in *Prx1cre;Twist1* mutant limb buds. (**A**) Forelimb buds from mouse embryos of the indicated genotypes and stages were used for western blot analysis with antibodies against TWIST1 and β-actin. In *Prx1cre;Twist1* mutant forelimb buds, TWIST1 protein is largely lost by E11. (**B-E**) Expression of *Fgf8* in E11 forelimb buds as analyzed by RNA in situ hybridization. C,E are enlarged distal views of B,D, respectively, with anterior up. (**F-M**) Expression of *Shh* in E10.5 (F-I) and E11 (J-M) forelimb buds as analyzed by RNA in situ hybridization. G,I,K,M are anterior views of F,H,J,L, respectively, with dorsal to the left. Arrows (H,I,LM) indicate the ectopic *Shh* domain. White dashed lines (I,M) indicate the anterior extent of the apical ectodermal ridge (AER). (**N-U**) Expression of *Gli1*, *Ptch1*, *Fgf4* and gremlin 1 in E11 forelimb buds as analyzed by RNA in situ hybridization. Arrows indicate anterior ectopic expression (O,Q) or the anterior extent of the respective expression domains (R-U).

(Buscher et al., 1997; Masuya et al., 1997; Qu et al., 1997; Zhang et al., 2009), *Prx1cre;Twist1* forelimb buds show ectopic *Shh* expression at an earlier stage of development and this expression extends to a larger domain.

Anterior *Shh* expression and related changes in SHH signaling were also observed in the limb buds of a hypomorphic allele of *Twist1*, *Twist1*$^{Ska10/Ska10}$ (see Fig. S3A-F in the supplementary material) (Bialek et al., 2004). In addition, ectopic SHH activity was detected in the hindlimb buds of heterozygous *Prx1cre;Twist1*$^{F/+}$ mutants, although the domain was smaller than that in the homozygous *Prx1cre;Twist1* mutants (see Fig. S3J-L in the supplementary material). Ectopic SHH activity was not detected in the forelimb buds of heterozygous *Prx1cre;Twist1*$^{F/+}$ mutants, although it was observed in the forelimb buds of

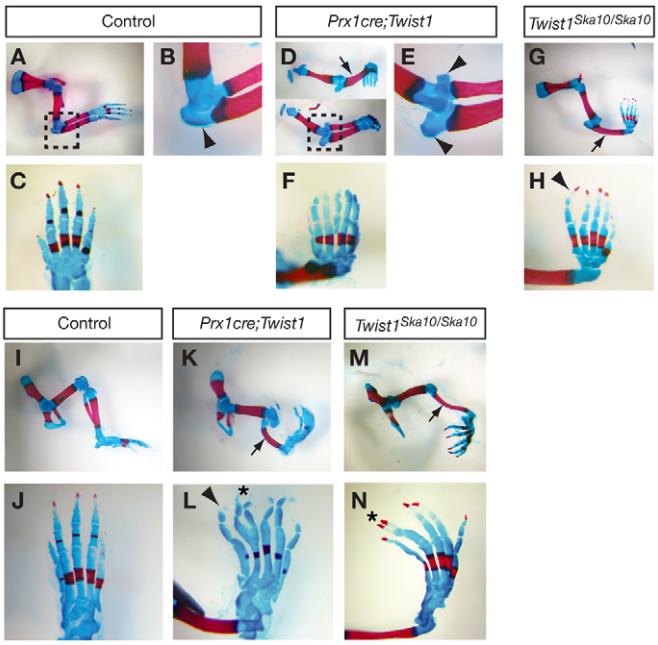

Fig. 2. Limb skeletal phenotypes of *Prx1cre;Twist1* and *Twist1*$^{Ska10/Ska10}$ mutants. (**A-N**) Skeleton preparations of mouse P1 forelimbs (A-H) and hindlimbs (I-N). Upper panel in D shows an example of a mutant forelimb lacking radius, whereas the lower panel shows an example of a mutant forelimb with radius-to-ulna transformation. The boxed regions in A,D are enlarged in B,E, respectively. Arrowheads indicate the olecranon process as a feature unique to the ulna (B,E), or a tri-phalanx anterior digit (H,L). Arrows (D,G,K,M) indicate the presence of only the posterior element in the zeugopod. Asterisks (L,N) indicate bifurcated digits. The autopod-only views in all figures are oriented with anterior to the left.

homozygous *Prx1cre;Twist1* mutants (see Fig. S3G-I in the supplementary material). These observations together suggest that TWIST1 is a major inhibitor of *Shh* expression in the limb bud, that it can act in a dose-dependent manner, and that the hindlimb bud is more sensitive to *Twist1* dosage than the forelimb bud.

Twist1 mutants exhibit limb skeletal phenotypes consistent with its role as an inhibitor of *Shh* expression

Whereas *Twist1*-null mutants die shortly after limb bud initiation (Chen and Behringer, 1995), both *Prx1cre;Twist1* and *Twist1*$^{Ska10/Ska10}$ mutants survive to birth, permitting analysis of their skeletal phenotypes. Both mutants displayed similar limb A-P patterning defects, as shown in the zeugopod and autopod (Fig. 2). In the forelimb zeugopod, all *Twist1*$^{Ska10/Ska10}$ (n=10) and a subset of the *Prx1cre;Twist1* limbs (n=4/8) exhibited radial agenesis, whereas the remainder of the *Prx1cre;Twist1* forelimbs exhibited radius-to-ulna transformation (Fig. 2A,B,D,E,G). In the hindlimb zeugopod, all mutant limbs exhibited tibial agenesis (n=8 for *Prx1cre;Twist1*; n=10 for *Twist1*$^{Ska10/Ska10}$; Fig. 2I,K,M). In the autopod of the forelimbs and hindlimbs, extra digits or bifurcation of digit tips was observed in all *Prx1cre;Twist1* limbs and a subset of *Twist1*$^{Ska10/Ska10}$ limbs (Fig. 2C,F,J,L,N). Furthermore, in contrast to the normal two-phalanx digit one identity, the most anterior digit in the mutants often adopted a posteriorized three-phalanx identity (Fig. 2H,L). These zeugopod and autopod defects have been observed in other mutants with ectopic anterior *Shh* expression (Charite et al., 2000; Sagai et al., 2004) and are thus consistent with the role of *Twist1* as an inhibitor of *Shh* expression.

Genetic interaction between Etv genes and *Twist1*

Following identification of *Twist1* as a negative regulator of *Shh* expression, we sought to address the relationship between Etv genes and *Twist1* in their roles as negative regulators of *Shh* expression in mouse limb buds. We primarily used an in vivo approach because there is currently no established cell line that faithfully recapitulates the molecular context of the developing limb bud. To test for possible genetic interactions in vivo, we generated compound mutants, analyzed limb skeletons in newborn pups and examined gene expression patterns in midgestation limb buds.

First, we tested for a possible interaction in *Etv5*$^{+/–}$;*Twist1*$^{Ska10/+}$ double-heterozygous mutants. Neither *Etv5*$^{+/–}$ nor *Twist1*$^{Ska10/+}$ forelimbs or hindlimbs showed any zeugopod defects. In the double heterozygotes, whereas the forelimb zeugopod remained normal, 27% of double-heterozygous mutants (n=13/48) exhibited tibial agenesis in one or both hindlimbs (Fig. 3A-C). This phenotype is reminiscent of the zeugopod phenotype in *Twist1*$^{Ska10/Ska10}$ and *Prx1cre;Twist1* mutant hindlimbs (Fig. 2K,M). We also examined the autopod for genetic interactions. Whereas *Twist1*$^{Ska10/+}$ heterozygous mutant hindlimbs exhibited a PPD phenotype, the forelimb autopods were normal. In ~9% (n=4/48) of the *Etv5*$^{+/–}$;*Twist1*$^{Ska10/+}$ double-heterozygous mutants, we observed extra preaxial digits in the forelimb (Fig. 3D-F). Even though this phenotype is found in a small number of samples, it is significant because extra digits are never detected in the forelimbs of *Etv5*$^{+/–}$ or *Twist1*$^{Ska10/+}$ single-heterozygous mutants. Furthermore, extra digits are never observed in the forelimbs of *Tcre;Etv4*$^{–/–}$;*Etv5*$^{F/–}$ or *Twist1*$^{+/–}$ mutants, in which the function of these genes is more severely disrupted (Bourgeois et al., 1998; Zhang et al., 2009). The manifestation of defects in the compound mutants indicates that mutations in Etv and *Twist1* interact synergistically.

To address whether the genetic interaction between Etv genes and *Twist1* represents a general phenomenon between Etv and other negative regulators of *Shh* expression, we generated *Etv5*$^{+/–}$;*Gli3*$^{Xt\text{-}J/+}$ double mutants. *Gli3*$^{Xt\text{-}J/+}$, a heterozygous mutant carrying a loss-of-function allele of *Gli3*, offers a sensitive genetic background as it has been shown to genetically interact with several other mutants that exhibit PPD phenotypes (Dunn et al., 1997; O'Rourke et al., 2002; Panman et al., 2005). In contrast to *Etv5*$^{+/–}$;*Twist1*$^{Ska10/+}$ mutants, we failed to observe any enhancement of defects in the zeugopod or autopod of *Etv5*$^{+/–}$;*Gli3*$^{Xt\text{-}J/+}$ mutants (n=0/37, Fig. 3G-L) as compared with *Gli3*$^{Xt\text{-}J/+}$ single mutants. This result therefore distinguishes *Twist1* from *Gli3* as a specific Etv cooperator.

To further address whether the Etv-*Twist1* interaction revealed by the skeletal phenotypes reflects their cooperation in the control of *Shh* expression, we examined the pattern of *Gli1* expression, a sensitive readout of SHH activity, in compound mutant forelimb buds. To increase the penetrance of the limb phenotypes, we inactivated both copies of *Etv5* during limb bud initiation using *Tcre* (Zhang et al., 2009; Perantoni et al., 2005), and one copy of *Etv4* and *Twist1* using their null alleles. As predicted, in *Tcre;Etv4*$^{+/–}$;*Etv5*$^{F/–}$;*Twist1*$^{+/–}$ compound mutants, we observed an increased penetrance of the forelimb PPD skeletal phenotype (n=3/8) as compared with *Etv5*$^{+/–}$;*Twist1*$^{Ska10/+}$ mutants (n=4/48). At the molecular level, aberrant *Gli1* expression was never observed in the forelimb buds of either *Tcre;Etv4*$^{+/–}$;*Etv5*$^{F/–}$ (n=5)

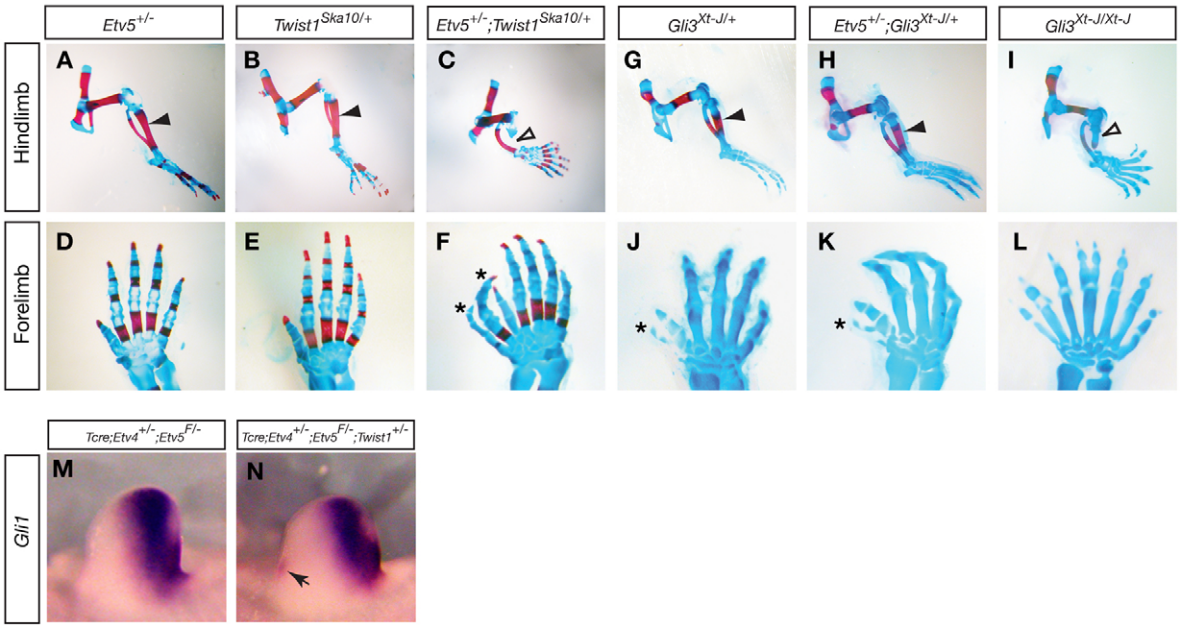

Fig. 3. Genetic interaction between Etv genes and *Twist1* in the limb. (**A-L**) Skeleton preparations of mouse P1 (A-F) or E16 (G-L) limbs of the indicated genotypes. Black arrowheads (B,G,H) indicate the presence of a normal tibia; white arrowheads (C,I) indicate truncated tibia. The hindlimb zeugopod phenotype in $Etv5^{+/-};Twist1^{Ska10/+}$ mutants (C) resembles that in *Prx1cre;Twist1* and $Twist1^{Ska10/Ska10}$ mutants (see Fig. 2K,M), and is more severe than that in $Etv5^{+/-}$ (A) or $Twist1^{Ska10/+}$ (B) mutants. The zeugopod remains normal in $Etv5^{+/-};Gli3^{Xt-J/+}$ mutants (H), similar to that in $Etv5^{+/-}$ (A) or $Gli3^{Xt-J/+}$ (G) mutants, but unlike that in $Gli3^{Xt-J/Xt-J}$ limbs (I) in which the tibia is shortened. Asterisks (F,J,K) indicate extra digit elements. The forelimb autopod phenotype in $Etv5^{+/-};Twist1^{Ska10/+}$ mutants (F) resembles that in *Prx1cre;Twist1* and $Twist1^{Ska10/Ska10}$ mutants (see Fig. 2F,H), and is more severe than that in $Etv5^{+/-}$ (D) or $Twist1^{Ska10/+}$ (E) mutants. The forelimb phenotype in $Etv5^{+/-};Gli3^{Xt-J/+}$ mutants (K) remains similar to that in $Gli3^{Xt-J/+}$ mutants (J), whereas in $Gli3^{Xt-J/Xt-J}$ mutants (L) the defect is more severe. (**M**,**N**) Expression of *Gli1* in E11 forelimb buds as analyzed by RNA in situ hybridization. Ectopic *Gli1* expression is detected in $Tcre;Etv4^{+/-};Etv5^{F/-};Twist1^{+/-}$ mutant forelimb buds (*n*=3/5; N, arrow), but not in $Tcre;Etv4^{+/-};Etv5^{F/-}$ mutants (M) (Mao et al., 2009; Zhang et al., 2009) or $Twist1^{+/-}$ mutant forelimb buds.

or $Twist1^{+/-}$ (*n*=7) mutants (Fig. 3M and data not shown) (Zhang et al., 2009). However, we detected ectopic *Gli1* expression in the anterior forelimb buds of $Tcre;Etv4^{+/-};Etv5^{F/-};Twist1^{+/-}$ mutants (*n*=3/5) (Fig. 3N). Together with the skeletal analysis data, these results support the possibility that Etv genes and *Twist1* interact synergistically to control A-P patterning and SHH activity in the limb bud.

Etv genes and *Twist1* are likely to function in the same genetic pathway to inhibit *Shh* expression in the limb bud

The genetic interaction between Etv and *Twist1* suggests that these genes might function either in parallel pathways or within a single pathway. To distinguish between these possibilities, we inactivated *Twist1* and both Etv genes in the entire limb bud mesenchyme by generating the homozygous compound mutant $Prx1cre;Etv4^{-/-};Etv5^{F/-};Twist1^{F/-}$ (hereafter *Prx1cre;Etv;Twist1*) and analyzed the expression of *Gli1* in these mutants. We reasoned that if Etv genes and *Twist1* act in parallel pathways to repress *Shh*, severe disruption of both Etv and *Twist1* should lead to more apparent ectopic SHH activity than in either mutant alone. However, if Etv genes and *Twist1* act within the same pathway, disruption of both Etv and *Twist1* should not lead to enhanced ectopic SHH activity. We found that in both *Prx1cre;Etv;Twist1* forelimb and hindlimb buds, there is no further expansion of the ectopic *Gli1* domain compared with either $Prx1cre;Etv4^{-/-};Etv5^{F/-}$ (hereafter *Prx1cre;Etv*) or *Prx1cre;Twist1* mutants (Fig. 4A-D and data not shown). These data are consistent with the possibility that Etv genes and *Twist1* act within the same pathway to repress SHH activity.

Etv genes and *Twist1* do not promote reciprocal expression in the limb bud

Recent data suggest that some *Shh* regulators act by controlling the expression of each other. For example, *Hand2* expression is upregulated in *Gli3* mutant limb buds, and GLI3 binds to the *Hand2* regulatory region, suggesting that GLI3 protein directly represses the transcription of *Hand2* (te Welscher et al., 2002; Vokes et al., 2008). Since our genetic data suggest that Etv genes and *Twist1* function in the same pathway, we tested whether they promote reciprocal expression by addressing if there is downregulation of expression in mutant limb buds. We found that in *Prx1cre;Twist1* mutant limb buds, the expression of *Etv4* and *Etv5* is not reduced, but rather slightly expanded anteriorly (Fig. 4E-H). This anterior spread is consistent with the findings that Etv genes serve as readouts of FGF signaling and that *Fgf4* expression is expanded in *Prx1cre;Twist1* mutant limb buds (Fig. 1S and see Fig. S1A-D in the supplementary material). Conversely, in *Tcre;Etv* limb buds, the expression of *Twist1* remained normal (Fig. 4I,J). These results suggest that Etv genes and *Twist1* do not act transcriptionally upstream or downstream of each other in A-P patterning.

ETV5 associates with TWIST1 in vitro and in vivo

We next tested the hypothesis that ETV and TWIST1 function by associating with one another at the protein level. First, we performed an in vitro pull-down assay to address whether ETV5 associates with TWIST1. Using His-tagged ETV5 expressed in *E. coli.* as bait, we were able to pull down TWIST1 protein from the lysate of HEK293T cells overexpressing *Twist1* (Fig. 5A). Second,

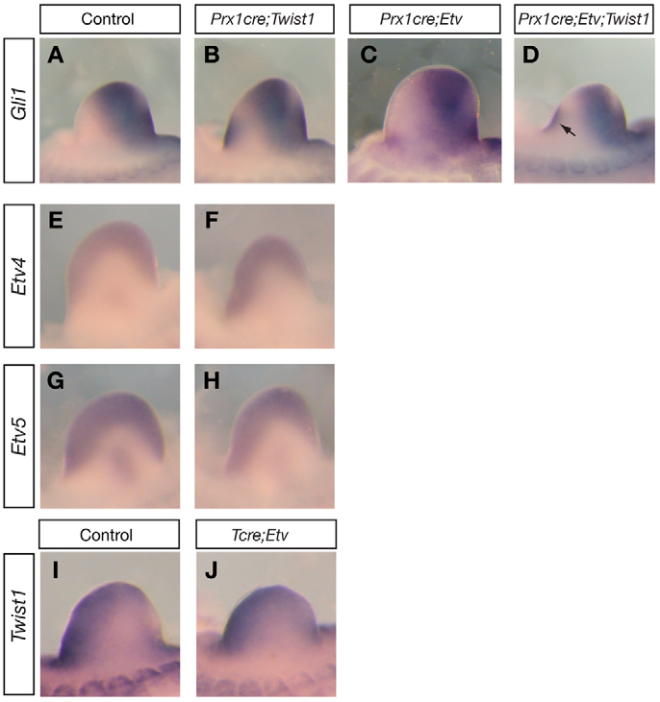

Fig. 4. Etv and *Twist1* are likely to function in the same genetic pathway but do not exhibit reciprocal control of expression. (**A-D**) Expression of *Gli1* in mouse E11 hindlimb buds as analyzed by RNA in situ hybridization. Compared with *Prx1cre;Twist1* mutants (B), the ectopic *Gli1* domain (arrow in D) in the *Prx1cre;Etv;Twist1* mutant is not expanded. (**E-H**) Expression of *Etv4* and *Etv5* in E11 forelimb buds as analyzed by RNA in situ hybridization. (**I**,**J**) Expression of *Twist1* in E11 hindlimb buds as analyzed by RNA in situ hybridization.

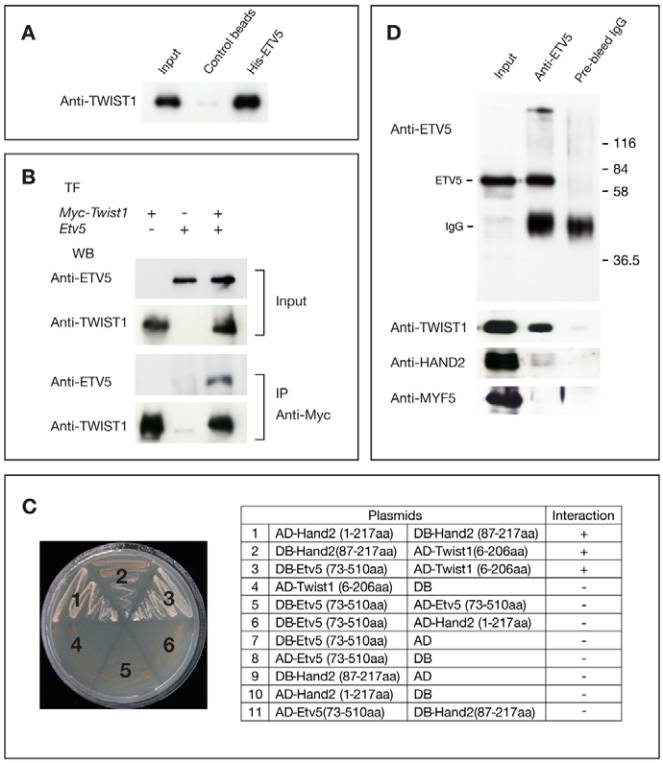

	Plasmids		Interaction
1	AD-Hand2 (1-217aa)	DB-Hand2 (87-217aa)	+
2	DB-Hand2(87-217aa)	AD-Twist1(6-206aa)	+
3	DB-Etv5 (73-510aa)	AD-Twist1 (6-206aa)	+
4	AD-Twist1 (6-206aa)	DB	-
5	DB-Etv5 (73-510aa)	AD-Etv5 (73-510aa)	-
6	DB-Etv5 (73-510aa)	AD-Hand2 (1-217aa)	-
7	DB-Etv5 (73-510aa)	AD	-
8	AD-Etv5 (73-510aa)	DB	-
9	DB-Hand2 (87-217aa)	AD	-
10	AD-Hand2 (1-217aa)	DB	-
11	AD-Etv5(73-510aa)	DB-Hand2(87-217aa)	-

Fig. 5. ETV5 and TWIST1 interact in vitro and in vivo. (**A**) In vitro pull-down assay showing that recombinant ETV5 can associate with TWIST1 in a cell lysate. Lysate from HEK293T cells transfected with Myc-tagged *Twist1* was incubated with either control Ni-NTA beads or Ni-NTA beads tethered with His-tagged ETV5 protein produced in *E. coli*. Western blot analysis of the pull-down samples using anti-TWIST1 antibody shows that TWIST1 protein efficiently associates with ETV5 beads, but not control beads. (**B**) Cell culture co-immunoprecipitation (CoIP) experiment showing that immunoprecipitation (IP) of TWIST1 can bring down ETV5 from the cell lysate. Lysate was prepared from HEK293T cells that were transfected with plasmids expressing either Myc-tagged *Twist1*, full-length *Etv5*, or both. IP was performed using anti-Myc antibody, and the product was analyzed by western blot using anti-ETV5 or anti-TWIST1 antibodies. The input lysate prior to IP was analyzed by western blot to show the presence of expressed proteins. (**C**) Yeast two-hybrid data showing that ETV5 can directly bind TWIST1 but not HAND2. The results (right) are from pairs of proteins in each test, fused to either the GAL4 activation domain (AD) or DNA-binding domain (DB). The plate (left) indicates the results from tests 1-6 in which transformed yeast cells were streaked onto medium lacking leucine, tryptophan and adenosine. Growth indicates protein interaction. As a control, all transformed strains grew on medium lacking just leucine and tryptophan. (**D**) In vivo CoIP data showing that IP of ETV5 from wild-type E11 limb bud lysate can bring down TWIST1 and HAND2. IP was performed using ETV5 antibody or pre-bleed IgG. The products were analyzed by western blot using antibodies against ETV5, TWIST1, HAND2 or MYF5. The ETV5 antibody is able to pull down TWIST1 and a small amount of HAND2, but not MYF5. TF, transfection; WB, western blot.

we carried out a co-immunoprecipitation (CoIP) assay in HEK293T cells. In cells overexpressing *Etv5* and Myc-tagged *Twist1*, we precipitated TWIST1 using an anti-Myc antibody. Western blot analysis of the immunoprecipitated product showed that ETV5 co-precipitates with TWIST1 (Fig. 5B). Third, we performed a yeast two-hybrid analysis. We found that ETV5 can interact with TWIST1 in this assay, consistent with the possibility that they can bind to each other directly (Fig. 5C). By contrast, ETV5 does not interact with itself, in agreement with previous data suggesting that PEA3 family transcription factors lack a homodimerization domain (Sharrocks, 2001).

Finally, to address whether the association between ETV5 and TWIST1 occurs in vivo, we carried out a CoIP assay using a polyclonal anti-ETV5 antibody that specifically recognizes both denatured and native ETV5 (Fig. 5D; see Fig. S4 in the supplementary material). We used this antibody to precipitate ETV5 from nuclear protein extracts of wild-type E11 limb buds. Compared with control pre-bleed IgG beads, the anti-ETV5 antibody-coupled beads pulled down ETV5, and together with it TWIST1 (Fig. 5D). By contrast, MYF5, another bHLH transcription factor expressed in limb buds, did not co-precipitate with ETV5. Together, these data indicate that ETV5 associates with TWIST1 in vitro and in vivo.

Etv interaction with *Hand2* in the limb bud

Recent CoIP and genetic data demonstrate that TWIST1 impacts limb A-P patterning by forming a protein heterodimer with, and antagonizing the function of, another bHLH factor, HAND2, which is a positive regulator of *Shh* (Charite et al., 2000; Fernandez-Teran et al., 2000; Firulli et al., 2005). Our yeast two-hybrid data also support the conclusion that TWIST1 and HAND2 are capable of direct interaction (Fig. 5C). Given our finding that ETV5 binds TWIST1, we asked whether ETV5 might also interact with HAND2.

A

Genotypes	2 ED + 2 ED	2 ED + 1 ED	2 ED	1 ED + 1 ED	1 ED	Normal
Tcre;Etv4$^{-/-}$*;Etv5*$^{F/-}$	5/12	2/12	1/12	3/12	1/12	0/12
Tcre;Etv4$^{-/-}$*;Etv5*$^{F/-}$*;Hand2*$^{F/+}$	0/6	0/6	0/6	0/6	1/6	5/6
Tcre;Etv4$^{+/-}$*;Etv5*$^{F/-}$	3/13	1/13	1/13	3/13	3/13	2/13
Tcre;Etv4$^{+/-}$*;Etv5*$^{F/-}$*;Hand2*$^{F/+}$	0/3	0/3	0/3	0/3	0/3	3/3

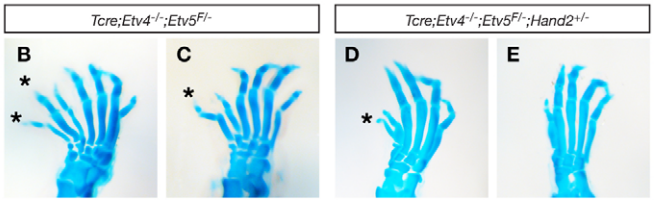

Fig. 6. Disruption of *Hand2* attenuates the Etv mutant limb phenotype. (**A**) A summary of hindlimb autopod phenotypes observed in E15.5 mouse embryos of the indicated genotypes. The fractions of embryos with either one or two extra digits (ED) in hindlimbs are listed. For example, the 2 ED + 1 ED column indicates fractions of animals with two extra digits on one hindlimb and one extra digit on the other hindlimb; the 2 ED column indicates fractions of animals with two extra digits on one hindlimb and no extra digit on the other hindlimb. A reduction of one copy of *Hand2* suppresses the preaxial polydactyly (PPD) phenotype of *Tcre;Etv* mutants. (**B-E**) Skeletal preparation of E15.5 hindlimbs representative of the more severe (B,D) versus the milder (C,E) phenotypes exhibited by limbs of the indicated genotypes. Of the six *Tcre;Etv4*$^{-/-}$*;Etv5*$^{F/-}$*;Hand2*$^{F/+}$ mutants that we examined, five showed normal hindlimbs, whereas the remaining one displayed a mild PPD phenotype as compared with *Tcre;Etv* mutants. Asterisks indicate anterior extra digits.

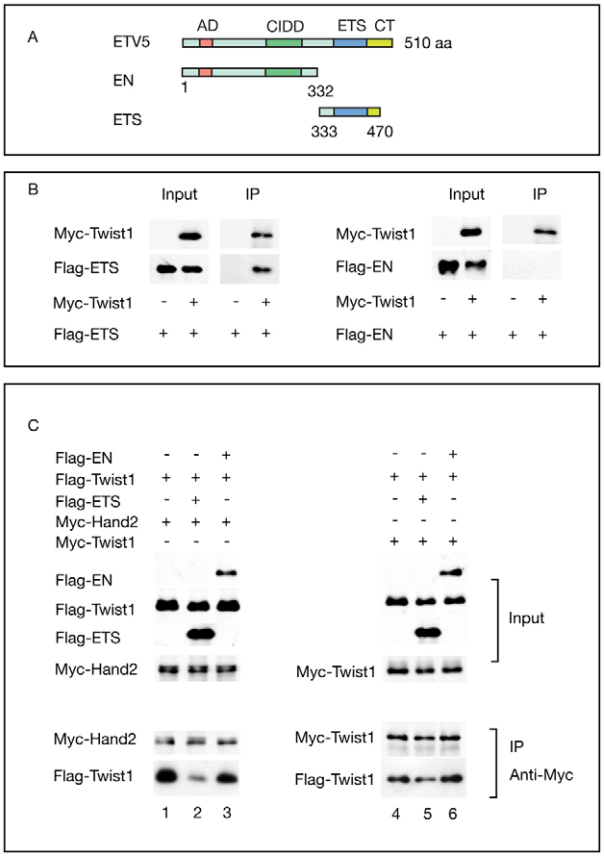

Fig. 7. ETV5 interferes with TWIST1-HAND2 dimerization. (**A**) Schematic representation of full-length and truncated ETV5. AD, acidic domain; CIDD, central inhibitory DNA-binding domain; CT, C-terminal tail. The numbers indicate the start and end amino acid positions of the truncated forms. (**B**) Cell culture CoIP experiments show that IP of TWIST1 can bring down Flag-ETS but not Flag-EN from the cell lysate. IP was performed using anti-Myc antibody, and the product was analyzed by western blot using anti-Flag antibody. (**C**) Cell culture CoIP experiments show that ETV5 inhibits TWIST1-HAND2 heterodimerization. IP was performed using anti-Myc antibody, and the product was analyzed by western blot using anti-TWIST1 (lanes 1-3) or anti-Flag (lanes 4-6) antibodies. As a control, in the absence of Myc-HAND2 or Myc-TWIST1 overexpression, no Flag-TWIST1 was co-precipitated using anti-Myc antibody (data not shown).

To address the genetic relationship between the two genes, we introduced a heterozygous loss-of-function mutant of *Hand2* (Morikawa et al., 2007) into *Tcre;Etv4*$^{-/-}$*;Etv5*$^{F/-}$, a mutant background in which we have previously studied the requirements for Etv in the limb. Consistent with what was shown previously (Zhang et al., 2009), all *Tcre;Etv4*$^{-/-}$*;Etv5*$^{F/-}$ mutants from this interaction mating exhibit a PPD phenotype in the hindlimb (Fig. 6A-C). However, the majority of *Tcre;Etv4*$^{-/-}$*;Etv5*$^{F/-}$*;Hand2*$^{F/+}$ mutants that we examined showed normal hindlimbs (Fig. 6A,D,E). This reduction in penetrance of the PPD phenotype indicates that lowering *Hand2* dosage attenuates the limb skeletal defect observed in Etv mutants.

We next addressed the biochemical relationship between ETV5 and HAND2. Yeast two-hybrid assays showed that ETV5 and HAND2 do not bind directly to each other (Fig. 5C), unlike ETV5 and TWIST1. In vivo CoIP tests showed that a small amount of HAND2 protein can be precipitated together with ETV5 (Fig. 5D). This result was obtained consistently from three CoIP experiments, whereas the negative control MYF5 was never detected in the pull-down. These data suggest that ETV5 might indirectly associate with HAND2 in the limb bud.

ETV5 inhibits TWIST1-HAND2 heterodimerization

Previous studies in the limb bud and other developmental settings have shown that different bHLH protein dimers exhibit distinct DNA binding specificities and transcriptional activities (Connerney et al., 2006; Firulli et al., 2007). Furthermore, in the limb bud, overexpression of TWIST1-HAND2 tethered dimers leads to a PPD phenotype, reminiscent of overexpression of the *Shh*-activator HAND2 alone (Firulli et al., 2007; Charite et al., 2000). By contrast, overexpression of TWIST1-TWIST1 tethered dimers leads to a phenotype that is reminiscent of *Shh* loss-of-function mutants (Chiang et al., 2001; Kraus et al., 2001; Lewis et al., 2001; Firulli et al., 2007). Point mutations in *Twist1* that affect its dimerization choice alter the effects of the resulting protein on limb skeletal patterning, suggesting that maintaining a precise balance of dimer species is essential for normal development (Firulli et al., 2007).

To further probe the mechanism underlying the genetic interactions among Etv, *Twist1* and *Hand2*, we addressed whether Etv regulates TWIST1 and HAND2 dimerization. In cultured cells, we found that a portion of the ETV5 protein containing the ETS DNA-binding domain (hereafter termed Flag-ETS) is capable of binding to TWIST1 (Fig. 7A,B). Binding was not observed between TWIST1 and the N-terminal portion of ETV5 that does not contain the ETS domain (hereafter termed Flag-EN).

Furthermore, we showed that the expression of Flag-ETS considerably reduces the amount of TWIST1 that is pulled down with HAND2 (Fig. 7C, columns 1, 2). A similar effect was not observed when Flag-EN is overexpressed (Fig. 7C, column 3). Finally, neither Flag-EST nor Flag-EN expression significantly altered the amount of Flag-TWIST1 that is pulled down with Myc-TWIST1 (Fig. 7C, columns 4-6). These data suggest that ETV5, probably through its ETS domain, interferes with TWIST1-HAND2 heterodimerization without having the same effect on TWIST1-TWIST1 homodimerization.

DISCUSSION

With the identification of multiple positive and inhibitory regulators of *Shh* expression in the limb bud, the current challenge is to decipher their functional relationship. In this study, we focused on three *Shh* expression regulators, Etv, *Twist1* and *Hand2*, and addressed the mechanism of their interaction. Using a conditional knockout strategy, we have shown that *Twist1* is required for preventing the expression of *Shh* in the anterior limb bud and for normal limb skeletal patterning. Data from compound mutants suggest that *Twist1*, Etv genes and *Hand2* function in the same genetic pathway. Furthermore, data from biochemical assays are consistent with the notion that they function via protein-protein interactions. Our findings highlight the importance of a precise balance between positive and inhibitory regulators of *Shh* expression in the control of limb A-P patterning.

In the majority of limb mutants in which it is misexpressed, *Shh* is detected ectopically in the anterior limb bud, separate from the normal domain in the posterior mesenchyme (Buscher et al., 1997; Qu et al., 1997; Zhang et al., 2009). The prevalence of this aberrant pattern led to the hypothesis that a distinct subset of cells in the anterior mesenchyme is poised to express *Shh*. This possibility is underscored by the observation that several positive regulators of *Shh* expression, including *Hand2*, *Tbx3* and *Pbx1*, are not only highly expressed in the posterior limb bud, but are also present, often in a separate domain, in the anterior proximal limb bud (Gibson-Brown et al., 1996; Charite et al., 2000; Capellini et al., 2006; Zakany and Duboule, 2007). We speculate that in a normal limb bud, these positive regulators are unable to activate *Shh* expression in the anterior mesenchyme because their function is inhibited by repressive machinery. Our findings suggest that the ETV-TWIST1 complex is a major component of this machinery, which in turn ensures the polarized posterior expression of *Shh*.

The question then arises as to why the presence of ETV and TWIST1 in the posterior limb bud is insufficient to inhibit *Shh* expression in the ZPA. This might be due in part to the fact that *Hand2*, a key positive regulator, is expressed much more intensely in the posterior than in the anterior mesenchyme (Charite et al., 2000; Galli et al., 2010). It is therefore plausible that although ETV and TWIST1 are present at a sufficient level to prevent HAND2 from activating *Shh* in the anterior limb bud, they are not abundant enough to do so in the posterior limb bud. In addition, there are negative regulators of *Shh* expression, such as ALX4, that are only present in the anterior mesenchyme (Qu et al., 1997). Their absence from the posterior mesenchyme might permit *Shh* expression in this domain.

Although *Twist1* and *Hand2* are the only bHLH genes that upon loss result in aberrant *Shh* expression, a number of other bHLH genes are expressed in the limb bud, including *E2a* (*Tcf3* – Mouse Genome informatics) and the Id genes. Besides forming heterodimers with each other, TWIST1 and HAND2 are each capable of interacting with E12 and E47, two isoforms encoded by the *E2a* gene (Firulli et al., 2005; Firulli et al., 2007). ID proteins, which do not contain DNA-binding domains, can also compete with TWIST1 and HAND2 for binding to E12/47 (Jogi et al., 2002). In vitro evidence suggests that different homo- or heterodimer pairs exhibit distinct DNA binding specificities and affinities (McFadden et al., 2002; Firulli et al., 2007). Moreover, the limb skeletal phenotypes that result from in vivo overexpression of tethered dimers suggest that different dimers might have distinct effects on *Shh* expression (Chiang et al., 2001; Kraus et al., 2001; Lewis et al., 2001; Firulli et al., 2007). For example, the similarity of phenotypes between TWIST1-HAND2 transgenics and HAND2-only transgenics suggests that TWIST1-HAND2 might positively regulate *Shh* expression. Conversely, the similarity of phenotypes between TWIST1-TWIST1 transgenics and *Shh* loss-of-function mutants suggest that TWIST1-TWIST1 might negatively regulate *Shh* expression. A recent study has shown that there are multiple predicted bHLH factor binding sites (E-boxes) in the *Shh* limb enhancer ZRS, and that HAND2 is capable of activating the ZRS via direct binding to regions containing a subset of these E-boxes (Galli et al., 2010). These findings illustrate a plausible mechanism by which bHLH factors may directly regulate *Shh* expression in the limb bud, and that normal limb patterning is dependent on a proper combination of bHLH dimers.

Given the crucial role of bHLH dimers, it is important to understand the control of their pairing and function. Recent data demonstrate that phosphorylation of bHLH factors significantly influences both their dimerization potential and DNA binding affinity (Firulli et al., 2005; Firulli et al., 2007). Few non-bHLH transcription factors have been shown to influence bHLH dimer function through direct binding. In embryonic cardiomyocytes, biochemical data show that FHL2, a LIM domain-containing transcription factor, binds HAND1 and influences HAND1-E12 dimer function (Hill and Riley, 2004). Data from our present study led us to propose that ETV proteins, probably through their ETS domain, bind directly to TWIST1. Furthermore, through the ETS domain, ETV might interfere with TWIST1 binding to HAND2. This model is not only supported by both genetic and biochemical results presented here, but is also compatible with previous findings that a similar phenotype (PPD) is observed in Etv mutants and in transgenics overexpressing TWIST1-HAND2 tethered dimers (Zhang et al., 2009; Firulli et al., 2007). In light of the evidence, it is plausible that ETV regulates limb patterning by modulating the bHLH dimer equilibrium.

The genetic and biochemical interactions between ETV and bHLH proteins, such as TWIST1 and HAND2, are likely to play important roles in other biological settings beyond limb development. Etv expression patterns overlap with *Twist1* in several other developing tissues, such as the somites, cardiac mesenchyme, pharyngeal and branchial arches (Fuchtbauer, 1995; Chotteau-Lelievre et al., 2001; Brent and Tabin, 2004; Vincentz et al., 2008). Furthermore, the expression of both Etv and *Twist1* is upregulated in breast cancer cells (Baert et al., 1997; Yang et al., 2004). Thus, the relationship revealed by the genetic and biochemical data shown in this study might represent a general mechanism of collaboration between these two classes of proteins.

Acknowledgements

We thank Dr Monica Justice for the *Twist1*^{ska10} mutant mice; Dr Malcolm Logan for the *Prx1cre* mice; Dr Mark Lewandoski for the *Tcre* mice; Drs Tony Firulli and Beth Firulli for discussions and *Twist1* and *Hand2* expression constructs; Dr Richard Harland, Dr Brigid Hogan, Dr Nobuyuki Itoh, Dr Qiufu

Ma and Dr Matthew Scott for providing plasmids from which RNA in situ probes were prepared; Dr John Fallon, Dr Marian Ros and members of the Sun laboratory for discussions and critical reading of the manuscript; and Amber Lashua for technical assistance. This work was supported by NIH grant HD30284 (to R.R.B.) and NIH grants HD045522 and HD045522-05S1 (to X.S.). Deposited in PMC for release after 12 months.

Competing interests statement
The authors declare no competing financial interests.

Supplementary material
Supplementary material for this article is available at
http://dev.biologists.org/lookup/suppl/doi:10.1242/dev.051789/-/DC1

References

Baert, J. L., Monte, D., Musgrove, E. A., Albagli, O., Sutherland, R. L. and de Launoit, Y. (1997). Expression of the PEA3 group of ETS-related transcription factors in human breast-cancer cells. *Int. J. Cancer* **70**, 590-597.
Bialek, P., Kern, B., Yang, X., Schrock, M., Sosic, D., Hong, N., Wu, H., Yu, K., Ornitz, D. M., Olson, E. N. et al. (2004). A twist code determines the onset of osteoblast differentiation. *Dev. Cell* **6**, 423-435.
Bourgeois, P., Bolcato-Bellemin, A. L., Danse, J. M., Bloch-Zupan, A., Yoshiba, K., Stoetzel, C. and Perrin-Schmitt, F. (1998). The variable expressivity and incomplete penetrance of the twist-null heterozygous mouse phenotype resemble those of human Saethre-Chotzen syndrome. *Hum. Mol. Genet.* **7**, 945-957.
Brent, A. E. and Tabin, C. J. (2004). FGF acts directly on the somitic tendon progenitors through the Ets transcription factors Pea3 and Erm to regulate scleraxis expression. *Development* **131**, 3885-3896.
Buscher, D., Bosse, B., Heymer, J. and Ruther, U. (1997). Evidence for genetic control of Sonic hedgehog by Gli3 in mouse limb development. *Mech. Dev.* **62**, 175-182.
Capellini, T. D., Di Giacomo, G., Salsi, V., Brendolan, A., Ferretti, E., Srivastava, D., Zappavigna, V. and Selleri, L. (2006). Pbx1/Pbx2 requirement for distal limb patterning is mediated by the hierarchical control of Hox gene spatial distribution and Shh expression. *Development* **133**, 2263-2273.
Charite, J., McFadden, D. G. and Olson, E. N. (2000). The bHLH transcription factor dHAND controls Sonic hedgehog expression and establishment of the zone of polarizing activity during limb development. *Development* **127**, 2461-2470.
Chen, Y., Knezevic, V., Ervin, V., Hutson, R., Ward, Y. and Mackem, S. (2004). Direct interaction with Hoxd proteins reverses Gli3-repressor function to promote digit formation downstream of Shh. *Development* **131**, 2339-2347.
Chen, Y. T., Akinwunmi, P. O., Deng, J. M., Tam, O. H. and Behringer, R. R. (2007). Generation of a Twist1 conditional null allele in the mouse. *Genesis* **45**, 588-592.
Chen, Z. F. and Behringer, R. R. (1995). twist is required in head mesenchyme for cranial neural tube morphogenesis. *Genes Dev.* **9**, 686-699.
Chiang, C., Litingtung, Y., Harris, M. P., Simandl, B. K., Li, Y., Beachy, P. A. and Fallon, J. F. (2001). Manifestation of the limb prepattern: limb development in the absence of sonic hedgehog function. *Dev. Biol.* **236**, 421-435.
Chotteau-Lelievre, A., Dolle, P., Peronne, V., Coutte, L., de Launoit, Y. and Desbiens, X. (2001). Expression patterns of the Ets transcription factors from the PEA3 group during early stages of mouse development. *Mech. Dev.* **108**, 191-195.
Connerney, J., Andreeva, V., Leshem, Y., Muentener, C., Mercado, M. A. and Spicer, D. B. (2006). Twist1 dimer selection regulates cranial suture patterning and fusion. *Dev. Dyn.* **235**, 1345-1357.
Davenport, T. G., Jerome-Majewska, L. A. and Papaioannou, V. E. (2003). Mammary gland, limb and yolk sac defects in mice lacking Tbx3, the gene mutated in human ulnar mammary syndrome. *Development* **130**, 2263-2273.
Dunn, N. R., Winnier, G. E., Hargett, L. K., Schrick, J. J., Fogo, A. B. and Hogan, B. L. (1997). Haploinsufficient phenotypes in Bmp4 heterozygous null mice and modification by mutations in Gli3 and Alx4. *Dev. Biol.* **188**, 235-247.
Fernandez-Teran, M., Piedra, M. E., Kathiriya, I. S., Srivastava, D., Rodriguez-Rey, J. C. and Ros, M. A. (2000). Role of dHAND in the anterior-posterior polarization of the limb bud: implications for the Sonic hedgehog pathway. *Development* **127**, 2133-2142.
Firulli, B. A., Krawchuk, D., Centonze, V. E., Vargesson, N., Virshup, D. M., Conway, S. J., Cserjesi, P., Laufer, E. and Firulli, A. B. (2005). Altered Twist1 and Hand2 dimerization is associated with Saethre-Chotzen syndrome and limb abnormalities. *Nat. Genet.* **37**, 373-381.
Firulli, B. A., Redick, B. A., Conway, S. J. and Firulli, A. B. (2007). Mutations within helix I of Twist1 result in distinct limb defects and variation of DNA binding affinities. *J. Biol. Chem.* **282**, 27536-27546.
Fuchtbauer, E. M. (1995). Expression of M-twist during postimplantation development of the mouse. *Dev. Dyn.* **204**, 316-322.
Furniss, D., Lettice, L. A., Taylor, I. B., Critchley, P. S., Giele, H., Hill, R. E. and Wilkie, A. O. (2008). A variant in the sonic hedgehog regulatory sequence (ZRS) is associated with triphalangeal thumb and deregulates expression in the developing limb. *Hum. Mol. Genet.* **17**, 2417-2423.
Galli, A., Robay, D., Osterwalder, M., Bao, X., Benazet, J. D., Tariq, M., Paro, R., Mackem, S. and Zeller, R. (2010). Distinct roles of Hand2 in initiating polarity and posterior Shh expression during the onset of mouse limb bud development. *PLoS Genet.* **6**, e1000901.
Gibson-Brown, J. J., Agulnik, S. I., Chapman, D. L., Alexiou, M., Garvey, N., Silver, L. M. and Papaioannou, V. E. (1996). Evidence of a role for T-box genes in the evolution of limb morphogenesis and the specification of forelimb/hindlimb identity. *Mech. Dev.* **56**, 93-101.
Gurnett, C. A., Bowcock, A. M., Dietz, F. R., Morcuende, J. A., Murray, J. C. and Dobbs, M. B. (2007). Two novel point mutations in the long-range SHH enhancer in three families with triphalangeal thumb and preaxial polydactyly. *Am. J. Med. Genet.* **143**, 27-32.
Hill, A. A. and Riley, P. R. (2004). Differential regulation of Hand1 homodimer and Hand1-E12 heterodimer activity by the cofactor FHL2. *Mol. Cell. Biol.* **24**, 9835-9847.
Jogi, A., Persson, P., Grynfeld, A., Pahlman, S. and Axelson, H. (2002). Modulation of basic helix-loop-helix transcription complex formation by Id proteins during neuronal differentiation. *J. Biol. Chem.* **277**, 9118-9126.
Kraus, P., Fraidenraich, D. and Loomis, C. A. (2001). Some distal limb structures develop in mice lacking Sonic hedgehog signaling. *Mech. Dev.* **100**, 45-58.
Lettice, L. A., Heaney, S. J., Purdie, L. A., Li, L., de Beer, P., Oostra, B. A., Goode, D., Elgar, G., Hill, R. E. and de Graaff, E. (2003). A long-range Shh enhancer regulates expression in the developing limb and fin and is associated with preaxial polydactyly. *Hum. Mol. Genet.* **12**, 1725-1735.
Lewis, P. M., Dunn, M. P., McMahon, J. A., Logan, M., Martin, J. F., St-Jacques, B. and McMahon, A. P. (2001). Cholesterol modification of sonic hedgehog is required for long-range signaling activity and effective modulation of signaling by Ptc1. *Cell* **105**, 599-612.
Livet, J., Sigrist, M., Stroebel, S., De Paola, V., Price, S. R., Henderson, C. E., Jessell, T. M. and Arber, S. (2002). ETS gene Pea3 controls the central position and terminal arborization of specific motor neuron pools. *Neuron* **35**, 877-892.
Logan, M., Martin, J. F., Nagy, A., Lobe, C., Olson, E. N. and Tabin, C. J. (2002). Expression of Cre Recombinase in the developing mouse limb bud driven by a Prxl enhancer. *Genesis* **33**, 77-80.
Maas, S. A. and Fallon, J. F. (2005). Single base pair change in the long-range Sonic hedgehog limb-specific enhancer is a genetic basis for preaxial polydactyly. *Dev. Dyn.* **232**, 345-348.
Mao, J., McGlinn, E., Huang, P., Tabin, C. J. and McMahon, A. P. (2009). Fgf-dependent Etv4/5 activity is required for posterior restriction of Sonic Hedgehog and promoting outgrowth of the vertebrate limb. *Dev. Cell* **16**, 600-606.
Masuya, H., Sagai, T., Moriwaki, K. and Shiroishi, T. (1997). Multigenic control of the localization of the zone of polarizing activity in limb morphogenesis in the mouse. *Dev. Biol.* **182**, 42-51.
McFadden, D. G., McAnally, J., Richardson, J. A., Charite, J. and Olson, E. N. (2002). Misexpression of dHAND induces ectopic digits in the developing limb bud in the absence of direct DNA binding. *Development* **129**, 3077-3088.
McGlinn, E. and Tabin, C. J. (2006). Mechanistic insight into how Shh patterns the vertebrate limb. *Curr. Opin. Genet. Dev.* **16**, 426-432.
Morikawa, Y., D'Autreaux, F., Gershon, M. D. and Cserjesi, P. (2007). Hand2 determines the noradrenergic phenotype in the mouse sympathetic nervous system. *Dev. Biol.* **307**, 114-126.
Neubuser, A., Peters, H., Balling, R. and Martin, G. R. (1997). Antagonistic interactions between FGF and BMP signaling pathways: a mechanism for positioning the sites of tooth formation. *Cell* **90**, 247-255.
Niswander, L. (2002). Interplay between the molecular signals that control vertebrate limb development. *Int. J. Dev. Biol.* **46**, 877-881.
O'Rourke, M. P., Soo, K., Behringer, R. R., Hui, C. C. and Tam, P. P. (2002). Twist plays an essential role in FGF and SHH signal transduction during mouse limb development. *Dev. Biol.* **248**, 143-156.
Panman, L., Drenth, T., Tewelscher, P., Zuniga, A. and Zeller, R. (2005). Genetic interaction of Gli3 and Alx4 during limb development. *Int. J. Dev. Biol.* **49**, 443-448.
Perantoni, A. O., Timofeeva, O., Naillat, F., Richman, C., Pajni-Underwood, S., Wilson, C., Vainio, S., Dove, L. F. and Lewandoski, M. (2005). Inactivation of FGF8 in early mesoderm reveals an essential role in kidney development. *Development* **132**, 3859-3871.
Qu, S., Niswender, K. D., Ji, Q., van der Meer, R., Keeney, D., Magnuson, M. A. and Wisdom, R. (1997). Polydactyly and ectopic ZPA formation in Alx-4 mutant mice. *Development* **124**, 3999-4008.
Qu, S., Tucker, S. C., Ehrlich, J. S., Levorse, J. M., Flaherty, L. A., Wisdom, R. and Vogt, T. F. (1998). Mutations in mouse Aristaless-like4 cause Strong's luxoid polydactyly. *Development* **125**, 2711-2721.

Sagai, T., Masuya, H., Tamura, M., Shimizu, K., Yada, Y., Wakana, S., Gondo, Y., Noda, T. and Shiroishi, T. (2004). Phylogenetic conservation of a limb-specific, cis-acting regulator of Sonic hedgehog (Shh). *Mamm. Genome* **15**, 23-34.

Sagai, T., Hosoya, M., Mizushina, Y., Tamura, M. and Shiroishi, T. (2005). Elimination of a long-range cis-regulatory module causes complete loss of limb-specific Shh expression and truncation of the mouse limb. *Development* **132**, 797-803.

Sharrocks, A. D. (2001). The ETS-domain transcription factor family. *Nat. Rev. Mol. Cell Biol.* **2**, 827-837.

Tarchini, B., Duboule, D. and Kmita, M. (2006). Regulatory constraints in the evolution of the tetrapod limb anterior-posterior polarity. *Nature* **443**, 985-988.

te Welscher, P., Fernandez-Teran, M., Ros, M. A. and Zeller, R. (2002). Mutual genetic antagonism involving GLI3 and dHAND prepatterns the vertebrate limb bud mesenchyme prior to SHH signaling. *Genes Dev.* **16**, 421-426.

Vincentz, J. W., Barnes, R. M., Rodgers, R., Firulli, B. A., Conway, S. J. and Firulli, A. B. (2008). An absence of Twist1 results in aberrant cardiac neural crest morphogenesis. *Dev. Biol.* **320**, 131-139.

Vokes, S. A., Ji, H., Wong, W. H. and McMahon, A. P. (2008). A genome-scale analysis of the cis-regulatory circuitry underlying sonic hedgehog-mediated patterning of the mammalian limb. *Genes Dev.* **22**, 2651-2663.

Yang, J., Mani, S. A., Donaher, J. L., Ramaswamy, S., Itzykson, R. A., Come, C., Savagner, P., Gitelman, I., Richardson, A. and Weinberg, R. A. (2004). Twist, a master regulator of morphogenesis, plays an essential role in tumor metastasis. *Cell* **117**, 927-939.

Zakany, J. and Duboule, D. (2007). The role of Hox genes during vertebrate limb development. *Curr. Opin. Genet. Dev.* **17**, 359-366.

Zeller, R., Lopez-Rios, J. and Zuniga, A. (2009). Vertebrate limb bud development: moving towards integrative analysis of organogenesis. *Nat. Rev. Genet.* **10**, 845-858.

Zhang, Z., Verheyden, J. M., Hassell, J. A. and Sun, X. (2009). FGF-regulated Etv genes are essential for repressing Shh expression in mouse limb buds. *Dev. Cell* **16**, 607-613.

Zuniga, A., Quillet, R., Perrin-Schmitt, F. and Zeller, R. (2002). Mouse Twist is required for fibroblast growth factor-mediated epithelial-mesenchymal signalling and cell survival during limb morphogenesis. *Mech. Dev.* **114**, 51-59.

Table S1. Primers used to generate yeast two-hybrid plasmids

Region	Primer (5′ to 3′)
Etv5 (73-510 aa)	Sense: CATATGTTTCAGTCTGATAACTTGGTGCTT Antisense: GGATCCTTAGTAAGCGAAGCCTTCGGT
Hand2 (1-217 aa)	Sense: CATATGATGAGTCTGGTGGGGGGCT Antisense: GGATCCTCACTGCTTGAGCTCCAGGG
Hand2 (87-217 aa)	Sense: CATATGGCCGGGCCTCCCGG Antisense: GGATCCTCACTGCTTGAGCTCCAGGGCCCA
Twist1 (6-206 aa)	Sense: CATATGTCCAGCTCGCCAGTCTCT Antisense: GGATCCCTAGTGGGACGCGGACAT
Twist1 (81-206 aa)	Sense: CATATGGGAGGCGGCGGCGGC Antisense: GGATCCCTAGTGGGACGCGGACATGGACCA